Electrochemistry Communications 48 (2014) 86–90

Contents lists available at ScienceDirect

Electrochemistry Communications

journal homepage: www.elsevier.com/locate/elecom

Short communication

Electrochemistry-assisted microstructuring of reduced graphene oxide-based microarrays with adjustable electrical behavior

Ming Zhao [a], Aiping Liu [a,b,*], Huaping Wu [c], Bingbing Wu [c], Chaorong Li [a], Weihua Tang [d]

[a] Center for Optoelectronics Materials and Devices, Zhejiang Sci-Tech University, Hangzhou 310018, China
[b] State Key Lab of Silicon Materials, Zhejiang University, Hangzhou 310027, China
[c] Key Laboratory of E&M (Zhejiang University of Technology), Ministry of Education & Zhejiang Province, Hangzhou 310014, China
[d] State Key Laboratory of Information Photonics and Optical Communication, Beijing University Posts and Telecommunications, Beijing 100876, China

ARTICLE INFO

Article history:
Received 21 July 2014
Received in revised form 17 August 2014
Accepted 28 August 2014
Available online 6 September 2014

Keywords:
Reduced graphene oxide microarrays
Electrochemistry-assisted microstructuring
Controllable conductivity
Electrochemical reduction

ABSTRACT

An electrochemistry-assisted microstructuring process is developed for fabricating well-aligned reduced graphene oxide (rGO)-based micropatterns on arbitrary substrates using a combined method of photolithography, electrochemical reduction and wet etching techniques. The dimension of special-shaped rGO microarrays localized in an insulating GO matrix is effectively adjusted by changing GO reduction time without multi-mask patterning. The increased conductivity of rGO micropatterns by several orders of magnitude is achieved by controlling GO thickness and reduction time. The electrochemical activity of rGO micropatterns as microarray electrodes is confirmed by using ferricyanide in aqueous solution as the redox probe. The present method could be a scalable technology to conventional photolithography for fabricating arbitrary rGO micropatterns in an insulating GO matrix for their potential applications in next generation electronic and electrochemical devices.

1. Introduction

Graphene with carbon atoms tightly packed into a two-dimensional honeycomb lattice is attractive for potential application in next generation electronic devices due to its fascinating physical properties including high carrier mobility, large electro-mechanical modulation and excellent flexibility [1]. Graphene-based microstructures are regarded as promising alternatives to silicon-based ones in future electronic devices [2]. Types of micropatterned graphene-based devices have been fabricated for signal acquisition, transmission and sensing [3–6]. Various attempts at graphene patterning by inkjet printing [7], transfer printing [8], photolithography [3,6], nanolithography [5,9,10] and solvent evaporation [11] have been reported and focused on graphene nanosheets. Among these, conventional photolithography method is multistep. Therefore, more efforts are needed to develop a scalable and simplified process to reduce overall processing time and steps, making photolithography more suitable for graphene-based micropatterns preparation for better electronic applications.

Additionally, reduced graphene oxide (rGO) is an alternative to graphene in constructing electronic devices requiring electronic band gaps [12]. The rGO patterns can be achieved via the deoxygenation of GO with epoxide and hydroxyl groups in basal planes and carboxylic and carbonyl groups in edge planes [13]. Many methods such as chemical, electrochemical and electric reductions, heat treatment and direct laser writing can decrease the proportion of oxygenated groups on GO to form rGO [4,11–18] and partially restore electrical conductivity, specially constructing conductive pathways of rGO in the insulating GO matrix [4,13,18]. Here, we propose a process of combining convenient lithography and electrochemistry method to generate well-defined rGO-based microarrays in the GO interconnection matrix on arbitrary substrates. To the best of our knowledge, there are few reports on patterning electrically conducting pathways of localized rGO in the GO matrix by an electrochemistry-assisted method. We also succeed to achieve controllable conductive and sized rGO microarrays with special shapes by changing localized GO thickness and reduction time without multi-mask patterning. The localized reduction and patterning method would be important in the design of electronic devices.

2. Experimental

2.1. Reagents

Graphite (50 μm) was purchased from Shanghai Carbon Co., Ltd. ITO-coated glass slides with sheet resistance of 8 Ω/square were supplied by Sigma. All other chemicals were of analytical grade and used without further purification. The water was obtained from a Millipore Q purification system (resistivity >18 MΩcm).

* Corresponding author at: Center for Optoelectronics Materials and Devices, Zhejiang Sci-Tech University, Hangzhou 310018, China. Tel./fax: +86 571 86843468.
E-mail addresses: liuaiping1979@gmail.com, liuap@zstu.edu.cn (A. Liu).

http://dx.doi.org/10.1016/j.elecom.2014.08.030
1388-2481/

2.2. rGO microarray preparation

The well-defined array was lithographically patterned on conductive ITO-coated glass slides through traditional lithography with a positive resist thickness about ~1.7 μm (Fig. 1a). A copper film was electrodeposited on a patterned ITO surface in a 0.2 M $CuSO_4$ solution at −1.0 V (vs. saturated calomel electrode, SCE) for 60 s in a three-electrode system with patterned ITO, platinum foil and SCE as working, counter and reference electrodes, respectively, by an electrochemical workstation (CHI 630D, USA). Then exfoliated GO aqueous solution (4 mg/mL) synthesized by the modified Hummer's method [19] was spin-coated on above substrate at 3000 rpm for 45 s each time and repeated two, five and nine times, respectively, to form a uniform and continuous GO layers with the thicknesses of about 20 nm, 60 nm and 140 nm (observed by atomic force microscopy). The localized GO layers contacting copper microwells were further selectively electrochemically reduced at −1.1 V [14] in a 0.2 M phosphate buffer solution (pH7.4) in the three-electrode system and the resulting sample was wet etched in a 1 M $FeCl_3$ solution for 15 min and in acetone for 1 h to remove copper and resist films, releasing GO film with rGO microarrays. After cleaning in deionized water, the film with rGO microarrays was scooped out and could be transferred to desired substrates such as ITO-coated glass, quartz, SiO_2/Si wafer and flexible substrate.

2.3. Characterization

Morphologies of rGO microarrays were observed by scanning electron microscopy (SEM, Hitachi S4800) and laser microscope (Keyence VK-X100). Raman spectra and mapping were acquired with a Thermo Fisher DXR Raman spectrometer using a He–Ne laser (λ = 632.8 nm). Four-point-probe conductivity measurements for rGO interdigitated electrode arrays were conducted using a Keithley 2400 Current/Voltage Source Meter with a probe station. The electrochemical behaviors of $Fe(CN)_6^{3-/4-}$ redox couple at rGO microarray electrodes were investigated in the 5 mM $K_3Fe(CN)_6$ and 1 M KCl mixed solution at different scan rates.

3. Results and discussion

The dimension of rGO arrays with special shape is effectively adjusted by changing localized GO reduction time without other supportive procedures such as multi-mask patterning. When the 60-nm-thick GO layer is electrochemically reduced for 7 s, the diameter of rGO disk arrays is about 25 μm (Fig. 1b), which is identical with that of lithographic pattern of copper film (25 μm in diameter). With the increase of reduction time, the GO region around rGO disks is continually reduced to rGO, resulting in extension outward of rGO arrays along the radial direction

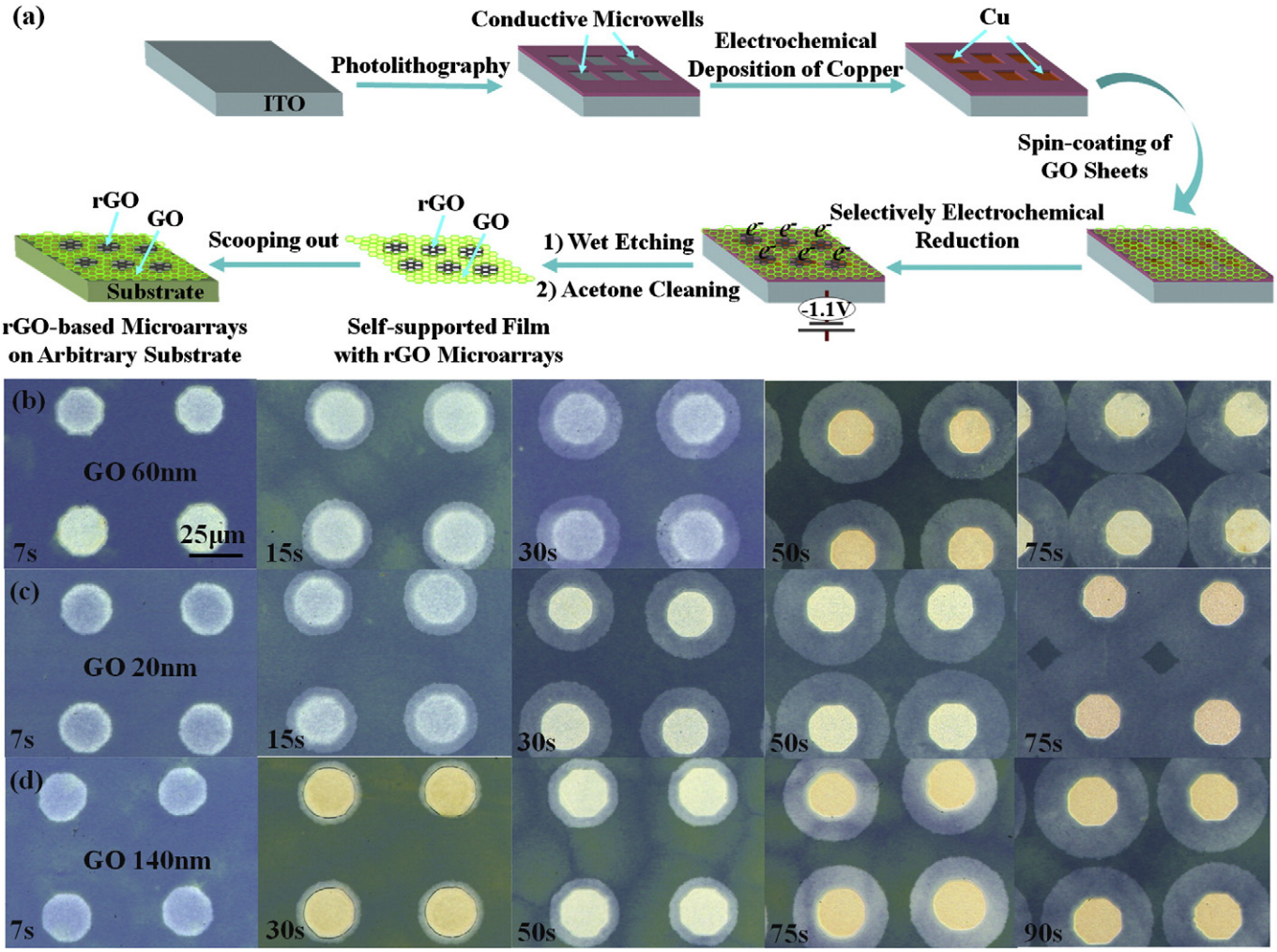

Fig. 1. (a) Schematic illustration of fabrication process of rGO-based microarrays in GO interconnection matrix. Laser microscope images of multi-thickness rGO-based microarrays on ITO-coated glass substrates with GO electrochemical reduction time of 7 s, 15 s, 30 s, 50 s, 75 s and 90 s, respectively: (b) 60-nm-thick GO, (c) 20-nm-thick GO and (d) 140-nm-thick GO. Scale bar is 25 μm.

of lithographic pattern (Fig. 1b). The color of extended rGO part is lighter than that of rGO one within the range of 25-μm diameter due to optical contrast arising from different reduced rGO parts. This reason will be discussed later. Until GO electrochemical reduction for 75 s, the boundary of each rGO disk overlaps. The diameter of rGO disk (D) and reduction time (T) are in line with $D = 0.43\,T + 25.03$ ($R = 0.995$). The slope demonstrates the reduction rate of 60-nm-thick GO along the radial direction of lithographic pattern is about 430 nm s^{-1}. Teoh et al. studied GO reduction process under a strong electric field and confirmed the importance of H^+ ions (resulting from ionized water molecules in air) in GO reduction [12]. When the GO sheet is spin-coated on the ITO substrate with the patterned copper film (as cathode electrode), GO reduction occurs on the copper surface at an extra potential (−1.1 V) by obtaining H^+ ions in ionized water molecules and electrons through conductive ITO and copper films. When GO reduction time exceeds 7 s, H^+ ions and electrons might be accumulated at the edge areas of rGO disks due to excellent electric conduction and high carrier mobility of rGO, resulting in further reduction of GO sheets on resist and diameter growth of rGO disks. Since 60-nm-thick GO reduction on the copper film is comparatively slow, the role of the copper film is of accelerating GO electrochemical reduction and constructing self-supported rGO–GO sheet after copper wet etching and resist removing. Additionally, we investigate the effect of GO thickness. When the 20-nm-thick GO is electrochemically reduced for 75 s, the boundary of each rGO disk has overlapped greatly (Fig. 1c), while the boundary overlapping of rGO has not occurred when the 140-nm-thick GO is reduced for 90 s (Fig. 1d). The linear relation between D and T is $D = 0.57\,T + 24.40$ ($R = 0.992$) for 20-nm-thick GO and $D = 0.34\,T + 22.72$ ($R = 0.996$) for 140-nm-thick GO, respectively. Therefore, the reduction rate of the thinner GO layer along the radial direction of the lithographic pattern is predominant.

We further design and obtain several rGO-based microarrays with different sizes and shapes by changing initial mold pattern and electrochemical reduction time of 60-nm-thick GO sheets (Fig. 2a–c). Well-aligned rGO disk arrays with a 10-μm diameter and square arrays with the areas of 80 μm × 80 μm and 20 μm × 20 μm, which are consistent with templates, can be obtained by controlling the GO reduction time of 15 s and 50 s, respectively. For the square arrays, the extension outward of rGO with the increasing of GO reduction time can be observed from Fig. 2d and e. Since the reduction rate of 60-nm-thick GO along the radial direction of the lithographic pattern (about 330 nm s^{-1}) is relatively constant, the resulting rGO arrays appear quasi-square when the boundary of each rGO square overlaps with the GO reduction time of 100 s (Fig. 1e). Fig. 2f shows the 3D-laser microscope image of disk arrays in Fig. 2a. The thickness of the edge area of the rGO disk is larger than those of rGO within 10-μm-diameter range and GO matrix. Fig. 2g shows the surface profile across several rGO disks, indicating thicker edges of rGO disks. In order to probe into the reason, the 3D-laser microscope image of copper microwells is given. It is found that the height of the electrodeposited copper film is larger than that of the resist layer and the edge area of copper microwells is thicker and rougher (Fig. 2h) due to the possibly higher current density induced by the edge effect. When the GO solution is spin-coated on the copper microwells, more GO sheets will stay at the rough edges and the microwells than on the resist. This results in relatively thicker edges for rGO micropatterns (Fig. 2f and g) and the optical contrast between the thinner extended rGO part and the slightly thicker rGO one within the range of diameter (Fig. 1b–d) when the localized GO layer is reduced to rGO.

The electrochemistry-assisted microstructuring is also confirmed by the change in Raman spectra before and after GO electrochemical reduction (Fig. 3a). The characteristic spectrum of the GO film on a SiO_2/Si substrate contains the G band (~1594 cm^{-1}) and the D band (~1345 cm^{-1}) [20]. The intensity ratio of D band to G band (I_D/I_G) increases from 0.93 for GO to 1.04, 1.15 and 1.21, respectively, after the 60-nm-thick GO electrochemical reduction for 15 s, 30 s and 50 s. This might be explained that the distortion of 6-membered rings caused by oxygen functionalities is removed after GO deoxidation, and the carbon lattice returns to an essentially graphitic state with highly defected, resulting in the increase of the I_D/I_G ratio [21]. Fig. 3b shows the intensity mapping of D band of rGO microarrays in Fig. 2d with the diameter of rGO element extended outward when the GO reduction time of 50 s. The Raman intensity of D peak is relatively uniform in the rGO part, which is lower than that of the D peak in the GO part and clearly distinguished from the surrounding GO areas, demonstrating precisely controlled locality of rGO patterns in reduction process. The effect of reduction time on conductive behavior of rGO on quartz substrates is investigated by four-point-probe electrical conductivity measurement on rGO interdigitated electrode arrays with a pitch of 50-μm width and 50-μm spacing between two pitches (Fig. 3c). The GO film is inherent insulating [22] with an electrical conductivity of 4.4×10^{-3} Sm^{-1}. The current–voltage (I–V) curves of 60-nm-thick rGO interdigitated electrodes in Fig. 4d exhibit linear behaviors over a voltage range from −1.5 to +1.5 V, which confirms the Ohmic behavior of rGO.

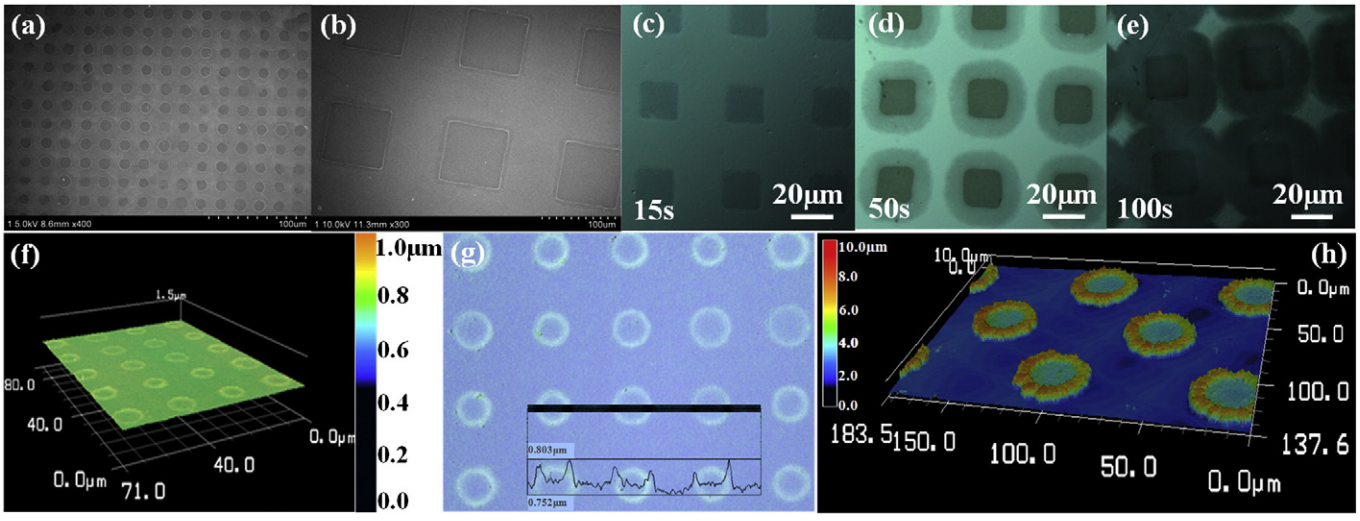

Fig. 2. SEM images of rGO microarrays on ITO-coated glass substrates: (a) 10-μm-diameter disks with 60-nm-thick GO reduction time of 15 s, (b) 80 μm × 80 μm squares with 60-nm-thick GO reduction time of 50 s. (c)–(e) Laser microscope images of 20 μm × 20 μm rGO square arrays on ITO-coated glass substrates with 60-nm-thick GO reduction time of (c) 15 s, (d) 50 s and (e) 100 s, respectively. (f) 3D-laser microscope image of disk microarrays in (a). (g) Surface profile across several rGO disks in (f). (h) 3D-laser microscope image of copper microwell arrays without a GO layer on their surfaces.

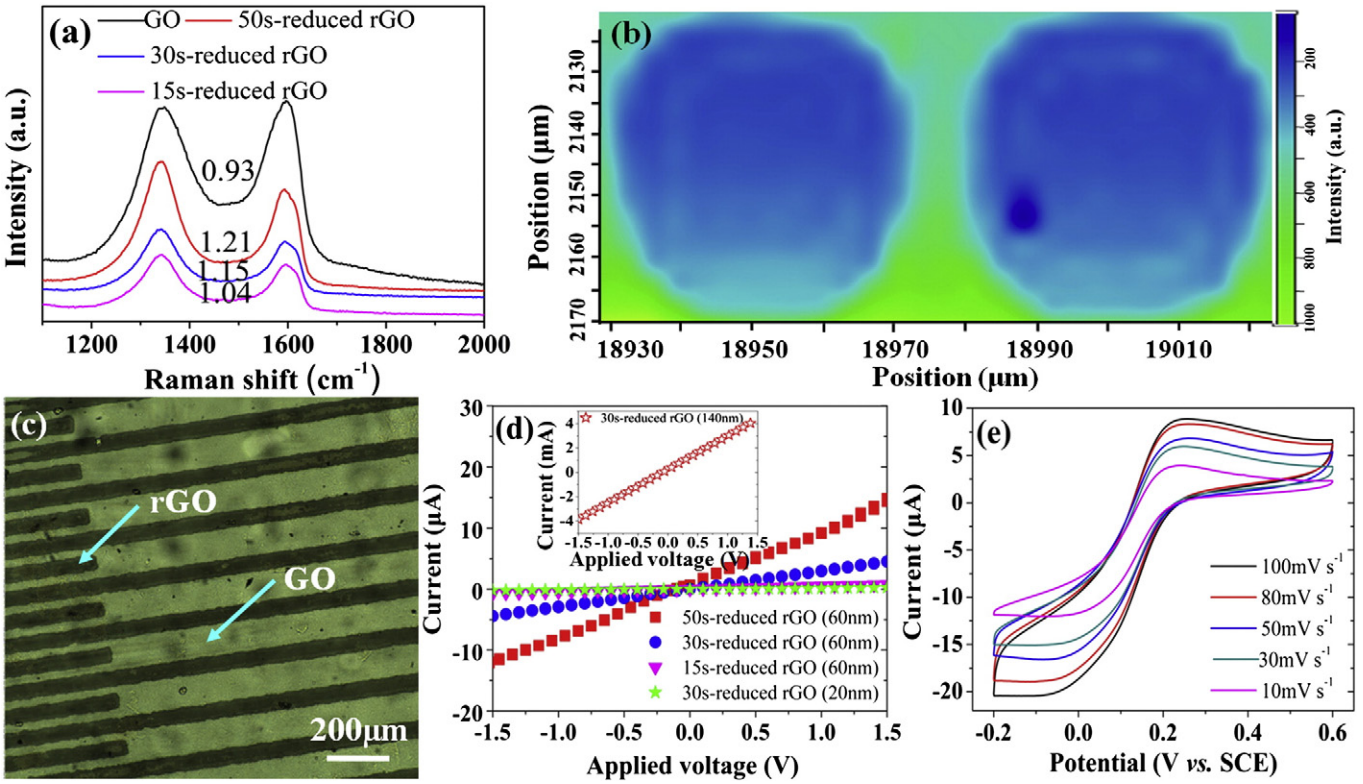

Fig. 3. (a) Raman spectra of 20 μm × 20 μm rGO square arrays before and after 60-nm-thick GO electrochemical reduction for different times, (b) Raman intensity mapping of D peak for rGO square arrays in Fig. 2d. (c) Microscope image of rGO interdigitated electrode arrays with a pitch of 50-μm width and 50-μm spacing between two pitches on quartz substrate with 60-nm-thick GO reduction time of 50s. (d) Current–voltage curves of multi-thickness rGO interdigitated electrode arrays with a GO reduction time of 15 s, 30 s and 50 s, respectively. (f) Cyclic voltammograms of 20 μm × 20 μm rGO square micropattern electrode (60-nm-thick GO is reduced for 15 s) in a 1 M KCl solution including 5 mM $K_3Fe(CN)_6$ at different scan rates.

Furthermore, the d*V*/d*I* values are also dependent on GO reduction time. The rGO conductivity increases dramatically with the increase of reduction time from 0 to 50 s. The high conductivity for 50 s-reduced rGO (about 42 Sm^{-1}) might be due to the reduction of oxygenated groups of GO [12]. The current variation of rGO after 50 s reduction is more sensitive than those of shorter-time reduced ones, meaning the controllable adjusting of electrical conductivity of rGO microarrays by changing GO reduction time. Furthermore, the thickness of rGO also greatly affects the conductive behavior of rGO. The 140-nm-thick rGO presents a higher conductivity about 4.1×10^3 Sm^{-1} compared to the 20-nm-thick (1.8 Sm^{-1}) and 60-nm-thick (9.9 Sm^{-1}) ones when the GO reduction time of 30 s. Therefore, the rGO micropatterns with a good electrical behavior can be obtained by reasonable controlling the thickness and reduction time of the localized GO layer. We further investigate the electrochemical property of $[Fe(CN)_6]^{3-/4-}$ redox couple at the rGO micropattern electrode shown in Fig. 2c. When the 60-nm-thick GO is reduced for 15 s, the reconstruction of essentially graphitic structure increases the electron transport of rGO, showing a good electrical conductivity and attendant high current response to $[Fe(CN)_6]^{3-/4-}$ reaction. The cyclic voltammograms of $[Fe(CN)_6]^{3-/4-}$ couple show a quasi-sigmoidal response at different scan rates (Fig. 3e), demonstrating the potential of rGO-based micropatterns fabricated with above method used as an electrochemical electrode.

4. Conclusions

An electrochemistry-assisted microstructuring process is developed for the fabrication of special-shaped rGO-based micropatterns with different feature sizes. The self-supported film with rGO microarrays in the GO interconnection matrix can be directly transferred to desired substrates and the dimension and conductivity of rGO microarrays can be effectively adjusted by controlling reduction time and thickness of the localized GO layer without multi-mask patterning. The present method provides a substantial possibility for the development of patterning strategies and extends the ability of conventional photolithography technology for the fabrication of arbitrary rGO micropatterns for their potential application in next generation electronic and electrochemical devices.

Conflict of interest

There is no conflict of interest.

Acknowledgments

This work was supported by the National Natural Science Foundation of China (Grant Nos. 51272237 and 11372280), the China Postdoctoral Science Foundation (Grant Nos. 2012M520063, 2013T60587 and Bsh1201016), the 521 Talent Project of Zhejiang Sci-Tech University, the Scientific Research Foundation for the Returned Overseas Chinese Scholars (State Education Ministry) (Grant No. 2013693) and the Technology Foundation for Selected Overseas Chinese Scholar of China (Grant No. 2012323).

References

[1] X. Huang, X. Qi, F. Boey, H. Zhang, Chem. Soc. Rev. 41 (2012) 666.
[2] Y. Zhou, K.P. Loh, Adv. Mater. 22 (2010) 3615.
[3] C.K. Huang, Y.X. Ou, Y.Q. Bie, Q. Zhao, D.P. Yu, Appl. Phys. Lett. 98 (2011) 263104.
[4] F.W. Li, M.Q. Xue, X.L. Ma, M.N. Zhang, Anal. Chem. 83 (2011) 6426.
[5] A.M.H. Ng, Y. Wang, W.C. Lee, C.T. Lim, K.P. Loh, H.Y. Low, Carbon 67 (2014) 390.
[6] S. Pang, H.N. Tsao, X. Feng, K. Müllen, Adv. Mater. 21 (2009) 3488.
[7] F. Torrisi, T. Hasan, W.P. Wu, Z.P. Sun, A. Lombardo, T.S. Kulmala, G.W. Hsieh, S.J. Jung, F. Bonaccorso, P.J. Paul, D.P. Chu, A.C. Ferrari, ACS Nano 6 (2012) 2992.
[8] L. Song, L.J. Ci, W. Gao, P.M. Ajayan, ACS Nano 3 (2009) 1353.
[9] Y.D. He, H.L. Dong, T. Li, C.L. Wang, W. Shao, Y.J. Zhang, L. Jiang, Appl. Phys. Lett. 97 (2010) 133301.

[10] C.X. Cong, T. Yu, Z.H. Ni, L. Liu, Z.X. Shen, W. Huang, J. Phys. Chem. C 113 (2009) 6529.
[11] T.Y. Kim, S.W. Kwon, S.J. Park, D.H. Yoon, K.S. Suh, W.S. Yang, Adv. Mater. 23 (2011) 2734.
[12] H.F. Teoh, Y. Tao, E.S. Tok, G.W. Ho, C.H. Sow, Appl. Phys. Lett. 98 (2011) 173105.
[13] Y. Zhou, Q.L. Bao, B. Varghese, L.A.L. Tang, C.K. Tan, C.H. Sow, K.P. Loh, Adv. Mater. 21 (2009) 1.
[14] A.P. Liu, T. Xu, Q.H. Ren, M. Yuan, W.J. Dong, W.H. Tang, Electrochem. Commun. 25 (2012) 74.
[15] Y. Matsumoto, M. Koinuma, S.Y. Kim, Y. Watanabe, T. Taniguchi, K. Hatakeyama, H. Tateishi, S. Ida, ACS Appl. Mater. Interfaces 2 (2010) 3461.
[16] I. Jung, D.A. Dikin, R.D. Piner, R.S. Ruoff, Nano Lett. 8 (2008) 4283.
[17] W. Gao, N. Singh, L. Song, Z. Liu, A.L. Reddy, L. Ci, R. Vajtai, Q. Zhang, B. Wei, P.M. Ajayan, Nat. Nanotechnol. 6 (2011) 496.
[18] D.E. Lobo, J. Fu, T. Gengenbach, M. Majumder, Langmuir 28 (2012) 14815.
[19] W.S. Hummers, R.E. Offeman, J. Am. Chem. Soc. 80 (1958) 1339.
[20] D. Graf, F. Molitor, K. Ensslin, C. Stampfer, A. Jungen, C. Hierold, L. Wirtz, Nano Lett. 7 (2007) 238.
[21] J.I. Paredes, S. Villar-Rodil, P. Solís-Fernández, A. Martínez-Alonso, J.M.D. Tascon, Langmuir 25 (2009) 5957.
[22] S. Stankovich, D.A. Dikin, R.D. Piner, K.A. Kohlhaas, A. Kleinhammes, Y.Y. Jia, Y. Wu, S. T. Nguyen, R.S. Ruoff, Carbon 45 (2007) 1558.